

Laser desorption/ionization from nanostructured surfaces: nanowires, nanoparticle films and silicon microcolumn arrays

Yong Chen¹, Guanghong Luo¹, Jiajie Diao², Olesya Chornoguz¹,
Mark Reeves^{2,3} and Akos Vertes^{1,3}

¹Department of Chemistry, The George Washington University, Washington, DC 20052

²Department of Physics, The George Washington University, Washington, DC 20052

³Institute for Proteomics Technology and Applications, The George Washington University, Washington, DC 20052

E-mail: vertes@gwu.edu

Abstract. Due to their optical properties and morphology, thin films formed of nanoparticles are potentially new platforms for soft laser desorption/ionization (SLDI) mass spectrometry. Thin films of gold nanoparticles (with 12 ± 1 nm particle size) were prepared by evaporation-driven vertical colloidal deposition and used to analyze a series of directly deposited polypeptide samples. In this new SLDI method, the required laser fluence for ion detection was equal or less than what was needed for matrix-assisted laser desorption/ionization (MALDI) but the resulting spectra were free of matrix interferences. A silicon microcolumn array-based substrate (a.k.a. black silicon) was developed as a new matrix-free laser desorption ionization surface. When low-resistivity silicon wafers were processed with a 22 ps pulse length $3\times\omega$ Nd:YAG laser in air, SF₆ or water environment, regularly arranged conical spikes emerged. The radii of the spike tips varied with the processing environment, ranging from approximately 500 nm in water, to ~ 2 μ m in SF₆ gas and to ~ 5 μ m in air. Peptide mass spectra directly induced by a nitrogen laser showed the formation of protonated ions of angiotensin I and II, substance P, bradykinin fragment 1-7, synthetic peptide, pro14-arg, and insulin from the processed silicon surfaces but not from the unprocessed areas. Threshold fluences for desorption/ionization were similar to those used in MALDI. Although compared to silicon nanowires the threshold laser pulse energy for ionization is significantly ($\sim 10\times$) higher, the ease of production and robustness of microcolumn arrays offer complementary benefits.

1. Introduction

Laser desorption/ionization mass spectrometry is a key method in the analysis of large biomolecules. The goal in these experiments is to efficiently produce ions from the molecules deposited on the surface of a substrate with minimal or controlled amount of fragmentation. It is also essential that the composition of the produced ions reflect the composition of the sample on the surface. In recent years, various methods of soft laser desorption/ionization (SLDI) have been developed to achieve this goal. The oldest and most successful version of the method, matrix-assisted laser desorption/ionization (MALDI), has been

demonstrated for different laser wavelengths (UV and IR) and various laser pulse lengths (ns, ps and fs pulses) [1, 2, 3]. Combined with mass spectrometry MALDI is capable of identifying biomolecules of moderate to large size (i.e., m/z 1,000 to 100,000). The presence of the organic matrix in MALDI, however, creates an obstacle in the analysis of small molecules, essential in a large number of applications (e.g., pharmaceuticals).

An alternative approach to optimizing the characteristics of the laser pulse is to adjust the properties of the desorption surface. By providing a nanoporous environment, desorption/ionization on amorphous silicon (DIOS) was the first method to offer interference free analysis in the low mass range [4]. In this contribution we report on experiments with new desorption surfaces including silicon nanowires [5], nanoparticle films and silicon microcolumn arrays (a.k.a. black silicon).

Submicron size particles, micro and nanostructured surfaces have been used to facilitate the desorption of large molecules. Early attempts included the use of ultrafine cobalt powder [6]. More recently, the utility of quasi-one dimensional systems, such as nanopores [4], nanowires [5] and nanotubes [7] have been demonstrated. Nanoparticles [8] are being studied to elucidate the possible role of the increased surface area and of uniquely nanoscopic phenomena, such as quantum confinement, liquid confinement and near-field effects. Beyond these random nanostructures lies the largely unexplored field of patterned nanostructures or nanoarrays that exhibit nanoscopic repeat units. Laser desorption/ionization investigations on these systems are just beginning. Ordered arrays of grooves [9] and cavities [10] on the nanoscale have been shown effective in the desorption and ionization of macromolecular ions of mostly small to medium size peptides.

In this paper we demonstrate that thin films produced by vertical colloidal deposition (VCD) [11] of gold nanoparticles can be successfully used in SLDI experiments. We also show that an array of sharp conical spikes can be induced by picosecond UV laser exposure of a silicon wafer in gas or liquid environment. The resulting surface covered by this ordered array, a.k.a. black silicon, has unique light absorption characteristics [12] and can be used as an efficient SLDI substrate. Finally, we compare the ion production characteristics of these two new desorption/ionization surfaces to the performance of silicon nanowires.

2. Experimental

2.1. Materials

Angiotensin I, substance P, leucine enkephalin, bradykinin, bovine insulin, ethanol, methanol and 2,5-dihydroxybenzoic acid (DHB) were obtained from Sigma Chemical Co. (St. Louis, MO). Reagent grade trifluoroacetic acid (TFA) was obtained from Aldrich (Milwaukee, WI). Stock solutions of the peptides were prepared at 10^{-3} M concentration in 0.1% TFA and diluted to 10^{-5} M for the SLDI experiments. The sulfur hexafluoride gas (SF_6) used in silicon wafer processing was obtained from Spectra Gases, Inc. (Branchburg, NJ). Acetonitrile solvent (HPLC grade) was purchased from Fisher Scientific (Springfield, NJ). Deionized water (18.2 M Ω /cm, produced by a D4631 E-pure system, Barnstead, Dubuque, IA) was used for the preparation of various solutions and for the laser processing of silicon wafers. All chemicals were used without further purification.

2.1. Nanoparticle film preparation

Thin films were fabricated on glass coverslips by self-assembly of spherical gold nanoparticles that were suspended in 0.02 weight percent colloidal solution. The nanoparticles themselves were 12 ± 1 nm in diameter and were synthesized by citrate reduction [13]. The self assembly was accomplished by VCD [11] at room temperature and at atmospheric pressure by immersing a clean glass cover slip vertically in the low-viscosity colloidal nanoparticle suspension. For VCD processing the substrate was coated by allowing the solvent (water) to evaporate. Due to interfacial forces nanoparticles at the liquid-air-substrate

interface were deposited in a continuous line on the substrate along the meniscus, which descended at a rate of $6 \mu\text{m}/\text{min}$ [11, 14]. A typical film deposited in this way was 100 nm thick, and had a resistivity of $10^{-5} \Omega\text{-m}$, about 1000 times that of pure gold.

2.2. Black silicon

In this study, we extended the original method to produce microstructured silicon surfaces by laser radiation. Earlier approaches were based on nanosecond [15] and femtosecond [16] laser irradiation with the latter focused on the visible spectral range. Her et al. noted that increasing the pulse length from 100 fs to 10 ps resulted in denser spike arrays and at 250 ps the spikes disappeared altogether [17]. In our work, a 22 ps mode-locked $3 \times \omega$ Nd:YAG laser was used at 355 nm for processing. Both positively (Si:B <100>) and negatively (Si:As <100>) doped, low resistivity ($\sim 0.001\text{--}0.005 \Omega\text{-cm}$) silicon wafers (University Wafer, South Boston, MA) were irradiated in air, SF_6 gas or deionized water. The wafers were cleaved to the desired size, cleaned sequentially with methanol and ethanol and finally air-dried. For processing, the clean silicon wafer was attached to the bottom of a Petri dish with double-sided tape and exposed to laser radiation in air or in deionized water. To produce the microstructures in SF_6 , the silicon wafer was placed in a small vacuum chamber that was evacuated to 1×10^{-2} Torr and backfilled with SF_6 gas to various pressures (1 to 500 Torr). The laser beam was focused to a ~ 1 mm diameter spot to produce $0.4\text{--}1.0 \text{ J}/\text{cm}^2$ fluence.

2.3. Surface morphology

A scanning electron microscope (SEM) (LEO 1460VP, Carl Zeiss, Thornwood, NY) and a transmission electron microscope (TEM) (JEOL 1200EX, Peabody, MA) were used to examine the produced micro and nanostructures. For TEM work, the gold film was floated off of the glass substrate and placed on a carbon-coated TEM grid. The TEM image was taken at an edge of the film where the sample was thin enough to resolve its microscopic structure. Typical results are shown in the left panel of figure 1 that demonstrates that the films are composed of uniformly distributed nanoparticles. These images, combined with the resistivity data indicate that the gold nanoparticles are loosely connected, but retain the shape and size that they originally had in the colloidal solution.

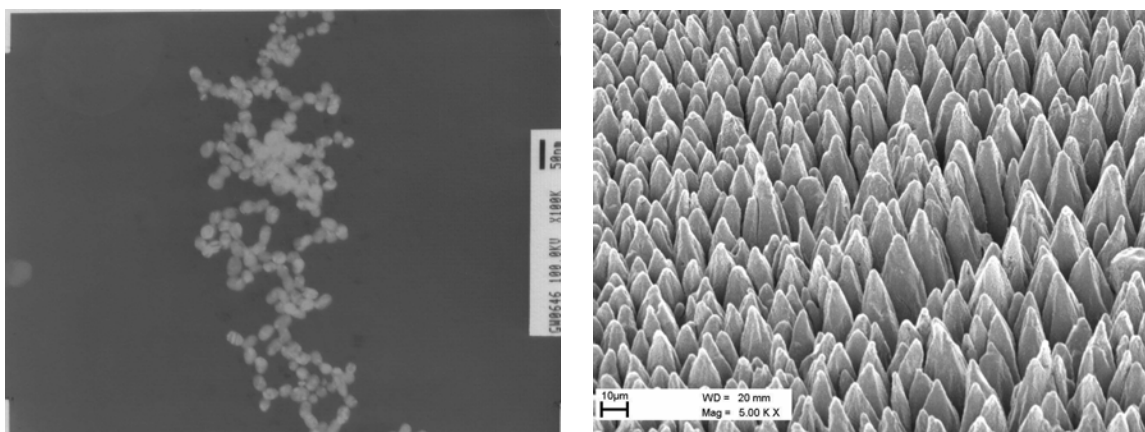


Figure 1. TEM image of gold nanoparticle film produced by VCD with 50 nm scale bar (left panel). SEM image of silicon microcolumn arrays produced in 10 Torr SF_6 with 1200 laser shots at 7 mJ: 45° view with $10 \mu\text{m}$ scale bar is shown in right panel.

Depending on the laser pulse energy, the focusing conditions and the environment, various morphologies were revealed by the SEM images. The wafer processed in ambient air with a 1000 shots of 7 mJ laser pulses exhibited deformations on its surface resulting in ubiquitous blunt protrusions. Among the protrusions, there were numerous holes that might have resulted from the burst of bubbles formed in an overheated subsurface silicon layer. At relatively low pressure (10 Torr), the SF₆ gas environment produced sharper and more regular protrusions on the surface resulting in arrays of spikes (see the right panel in figure 1). These features were 1-3 μm in diameter at the tip and measured 10-20 μm in height. The density and size of the spikes varied with the laser intensity distribution across the beam, with coarse, tall spikes in the center, and fine, short ones at the rim. In water, the spikes were less than 500 nm in diameter at the tips and less than 3 μm in height. The significantly finer structure might be attributed to the fast solidification of molten silicon due to the high thermal conductivity and high heat capacity of water.

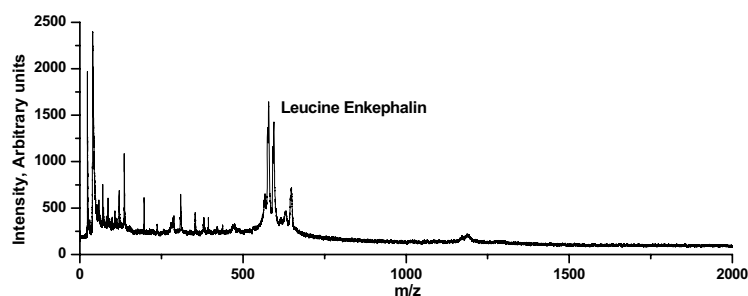
2.4. Laser desorption experiments

A home-built linear time-of-flight (TOF) mass spectrometer was used for the laser desorption studies. The detailed description of the instrument can be found elsewhere [2]. Briefly, ions generated with a 4 ns pulse length nitrogen laser at 337 nm (VSL-337ND, Laser Science Inc., Newton, MA) were accelerated to 25 keV and their flight time was recorded with a 1.5-GHz digital oscilloscope (LC684DXL, LeCroy, Chestnut Ridge, NY). A variable attenuator (935-5-OPT, Newport, Fountain Valley, CA) was used to adjust the laser fluence. Laser energy was measured with a pyroelectric joule meter (Model J4-05, Moletron, Portland, OR) and displayed by an energy meter (Energy Max 400, Moletron). The focal area of the laser beam was determined by measuring the burn mark on a photographic paper. For the SLDI experiments, 0.5 to 1.0 μl of the 10⁻⁵ M analyte solution analyte was deposited on the studied surface and air dried before spectrum collection.

3. Results and discussion

3.1 Nanoparticle films

Due to their optical properties and morphology, thin films formed of nanoparticles are potentially new platforms for SLDI mass spectrometry. Thin films of gold nanoparticles (with 12±1 nm particle size) were prepared by VCD and used to analyze a series of directly deposited polypeptide samples. Mass spectra of leucine enkephalin (556 Da), bradykinin (1060 Da) (see figure 2), angiotensin I (1296 Da) and substance P (1348 Da) (not shown) were recorded with good signal quality (S/N > 30). The laser energy range was between 3 and 4 μJ/pulse, whereas the required laser fluence for ion detection was equal or less than what was needed for MALDI. In contrast to MALDI the resulting spectra were free of matrix interferences.



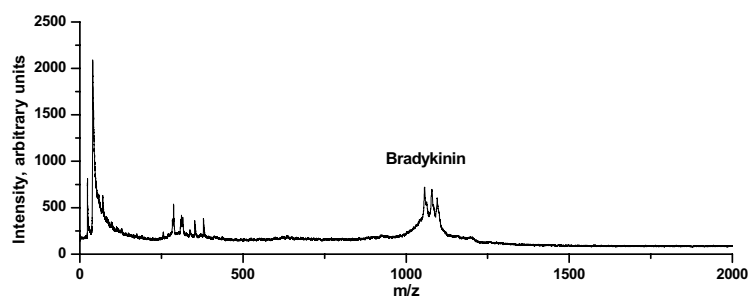


Figure 2. Mass spectra of leucine enkephalin (top) and bradykinin (bottom) produced by SLDI from gold nanoparticle films.

In an earlier study, McLean et al. used size selected colloidal gold nanoparticles in the 2 to 10 nm size range to generate peptide ions in SLDI experiments [8]. Their preparation was based on mixing the gold colloid with the peptide solution followed by dispensing a droplet onto the substrate and drying it in ambient air. This preparation resulted in very high laser energy requirements of $\sim 120 \mu\text{J}/\text{pulse}$ and in the presence of abundant gold cluster ions in their spectra. Our film preparations required 30 to 40 times lower laser pulse energy for peptide ion production. This resulted in significantly reduced energy transfer both to the gold particles and to the adsorbates. A clear consequence of the lower laser energy was that our spectra were free of gold cluster ions.

Another advantage of the gold films is their robustness. While aggregation can dramatically change the particle size in colloidal solutions and the corresponding ion yield in SLDI, the films produced by VCD are chemically and morphologically stable. This added stability also means that these films can be integrated into chip-based analytical devices.

3.1. Black silicon

Peptides and peptide mixtures were used in the SLDI experiments utilizing the black silicon described in section 2.3 as desorption surfaces. The spectra of various peptides indicated predominantly protonated ions up to $m/z \sim 6000$. The submicron tip diameter microcolumn arrays produced in water demonstrated the highest ion yields [18]. The threshold fluence at $\sim 30 \text{ mJ}/\text{cm}^2$ was comparable to values observed in MALDI. Figure 3 shows the SLDI spectrum of a three-component peptide mixture.

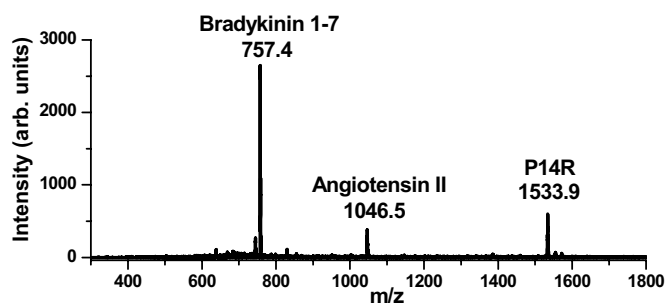


Figure 3. SLDI mass spectrum of a peptide mixture containing bradykinin fragment 1-7, angiotensin II and a synthetic peptide, pro14-arg, from a black silicon surface.

Although other silicon nanostructures, such as nanopores [4] and nanowires [5], are also used to produce peptide ions in SLDI experiments, the black silicon surfaces are significantly simpler to produce and can be more readily integrated into micro-chemical chips. Due to the uniform light absorption characteristics of the surface from near UV to mid IR, it is expected that a wide variety of lasers can be used for SLDI experiments.

Our earlier SLDI studies on 40-nm diameter and $\sim 1\text{-}\mu\text{m}$ long silicon nanowires with 10-50 wires/ μm^2 surface density indicated very low (0.3 $\mu\text{J/pulse}$) laser pulse energy requirements for ion production [5]. However, SEM studies on these surfaces revealed that the exposure of these quasi-one dimensional structures even to this extremely low laser radiation resulted in the evaporation of all the exposed nanowires. Thus, SLDI spectrum collection from a particular spot destroyed the surface and resulted in increasingly poor shot-to-shot reproducibility.

The SLDI procedures reported here for silicon microcolumn arrays were not optimized to give the highest ion yields. After processing, the surface of the black silicon was left in its native state. Thus, depending on the environment and ablation conditions, a varying degree of surface oxidation with a certain density of hydroxide groups was present. Further improvements are expected from refinements in surface preparation, including the optimization of laser processing conditions and the derivatization of the processed silicon surface. For example, to modify the wetting properties and the surface adsorbate interaction energies, the microcolumn arrays can be silylated.

4. Conclusions

Two new finely structured surfaces were introduced for SLDI. Compared to a suspension of gold nanoparticles used as a matrix, nanoparticle films produced by VCD offered a significantly (30–40 \times) reduced laser pulse energy requirement for SLDI of small peptides. Picosecond laser microstructuring of silicon resulted in a robust surface also capable of SLDI for peptide mixtures. These silicon surfaces were simple to produce and offered a great variety of potential chemical modifications. Although compared to silicon nanowires the threshold laser pulse energy for ionization was significantly ($\sim 10\times$) higher, the ease of production and robustness of microcolumn arrays offered complementary benefits.

Both the VCD method for nanoparticle film formation and the picosecond laser microstructuring of silicon present new directions in the preparation of “designer” surfaces for SLDI. With VCD, a large variety of nanoparticles can be assembled into thin films of varying surface density. Reducing the gold particle size below ~ 3 nm enables testing for the presence of quantum confinement effects in SLDI. The delicate control over the surface density of particles in VCD allows the production of submonolayer, monolayer and multilayer coverage. Thus, the effect of particle density on SLDI can be examined.

Silicon microcolumn arrays can be produced with a wide spectrum of morphologies by varying the aspect ratio, the density and the tip diameter of the columns. The column surfaces can be derivatized to alter their wetting properties and the interaction energy between the adsorbate and the surface.

Acknowledgements

The silicon nanowire samples were made available by G. Siuzdak of the Scripps Research Institute, La Jolla, CA, and by Nanosys Inc., Palo Alto, CA. Funding for this research was provided by grants from the US. Department of Energy (DE-FG02-01ER15129), the W. M. Keck Foundation (041904) and the George Washington University Research Enhancement Fund (GWU-REF). Support from the Department of Energy does not constitute an endorsement of the views expressed in the article.

References

- [1] Vertes A, Luo G, Ye L, Chen Y and Marginean I 2004 *Appl. Phys. A* **4-6** 823
- [2] Chen Y and Vertes A 2003 *J. Phys. Chem. A* **107** 9754

- [3] Papantonakis M R, Kim J, Hess W P and Haglund Jr R F 2002 *J. Mass Spectrom.* **37** 639
- [4] Wei J, Buriak J M and Siuzdak G 1999 *Nature* **399** 243
- [5] Go E P, Apon J V, Luo G, Saghatelian A, Daniels R H, Sahi V, Dubrow R, Cravatt B F, Vertes A and Siuzdak G 2005 *Anal. Chem.* **77** 1641
- [6] Tanaka K, Waki H, Ido Y, Akita S, Yoshida Y and Yoshida T 1988 *Rapid Commun. Mass Spectrom.* **2** 151
- [7] Xu S, Li Y, Zou H, Qiu J, Guo Z and Guo B 2003 *Anal. Chem.* **75** 6191
- [8] McLean J A, Stumpo K A and Russell D H 2005 *J. Am. Chem. Soc.* **127** 5304
- [9] Okuno S, Arakawa R, Okamoto K, Matsui Y, Seki S, Kozawa T, Tagawa S and Wada Y 2005 *Anal. Chem.* **77** 5364
- [10] Finkel N H, Prevo B G, Velev O D and He L 2005 *Anal. Chem.* **77** 1088
- [11] Diao J J, Qiu F S, Chen G D and Reeves M E 2003 *J. Phys. D Appl. Phys.* **36** L25
- [12] Wu C, Crouch C H, Zhao L, Carey J E, Younkin R, Levinson J A, Mazur E, Farrell R M, Gothoskar P and Karger A 2001 *Appl. Phys. Lett.* **78** 1850
- [13] Freeman R G, Hommer M B, Grabar K C, Jackson M A and Natan M J 1996 *J. Phys. Chem.* **100** 718
- [14] Diao J J, Hutchison J B, Luo G and Reeves M E 2005 *J. Chem. Phys.* **122** 184710
- [15] Rothenberg J E and Kelly R 1984 *Nucl. Instrum. Meth. Phys. Res.* **B1**, 291
- [16] Her T-H, Finlay R J, Wu C, Deliwala S and Mazur E 1998 *Appl. Phys. Lett.* **73** 1673
- [17] Her T-H, Finlay R J, Wu C and Mazur E 2000 *Appl. Phys. A* **70** 383
- [18] Chen Y and Vertes A 2006 *Anal. Chem.*, Web Release Date: 13-Jul-2006; DOI: [10.1021/ac060405n](https://doi.org/10.1021/ac060405n)